

KOPIO TN0XX draft  
More on the beam aspect ratio and FastMC  
acceptance

David E. Jaffe, BNL

April 2, 2003

**Abstract**

This document is a supplement to TN053. See TN053 for definitions of terms and variables.

## 1 Comparison of tails of distributions

Figures 1, 2, 3, 4 and 5 shows the fraction of the  $M(\gamma\gamma)$ ,  $P^*(\pi^0)$ ,  $Z(K)$ ,  $E(\gamma)$  and  $E^*(\gamma)$  distributions outside three  $\sigma$  where  $\sigma =$  core resolution from the resolution fits described in TN053. Technically, the fraction is defined as the contents of all bins with centers greater than  $3\sigma$  from the fitted mean divided by the total contents of the each histogram, thus there may be binning effects when  $\sigma$  is comparable to the bin size. The error bars show the binomial error.

For  $E(\gamma)$  and  $E^*(\gamma)$ , the tail fractions are comparable for the Zeller and Konaka PR models. The tail fractions for  $M(\gamma\gamma)$  are nearly twice as large with the Zeller PR model compared to the Konaka PR model. For  $P^*(\pi^0)$  and  $Z(K)$ , the tail fraction is  $\sim 50\%$  larger with the Zeller PR model.

2003/03/31 21.33

2003/03/31 21.33

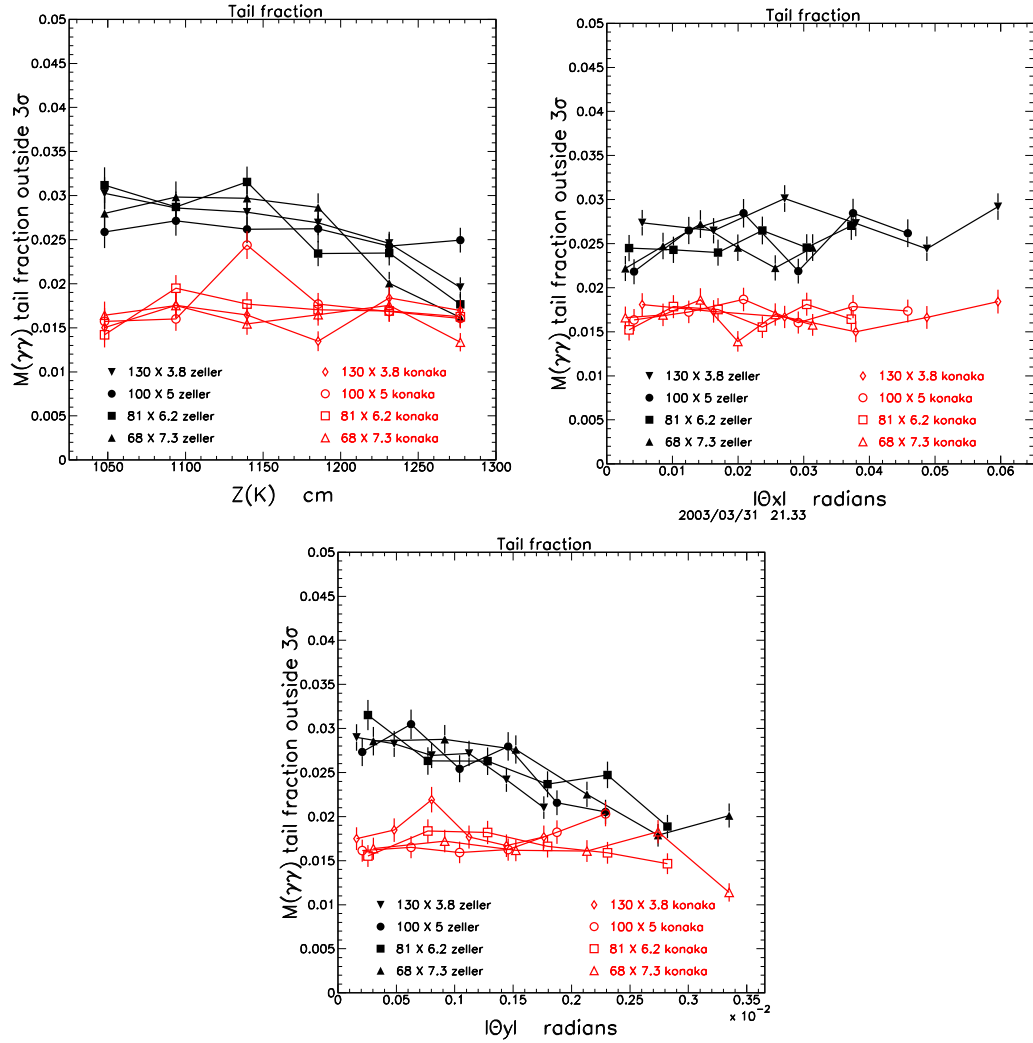


Figure 1: Fraction of  $M(\gamma\gamma)$  distribution outside three  $\sigma$  where  $\sigma =$  core resolution as a function of  $Z(K)$ ,  $|\Theta_X|$  and  $|\Theta_Y|$  for the Konaka and Zeller PR models for the four different beam aspect ratios after application of basic cuts.

2003/03/31 21.33

2003/03/31 21.33

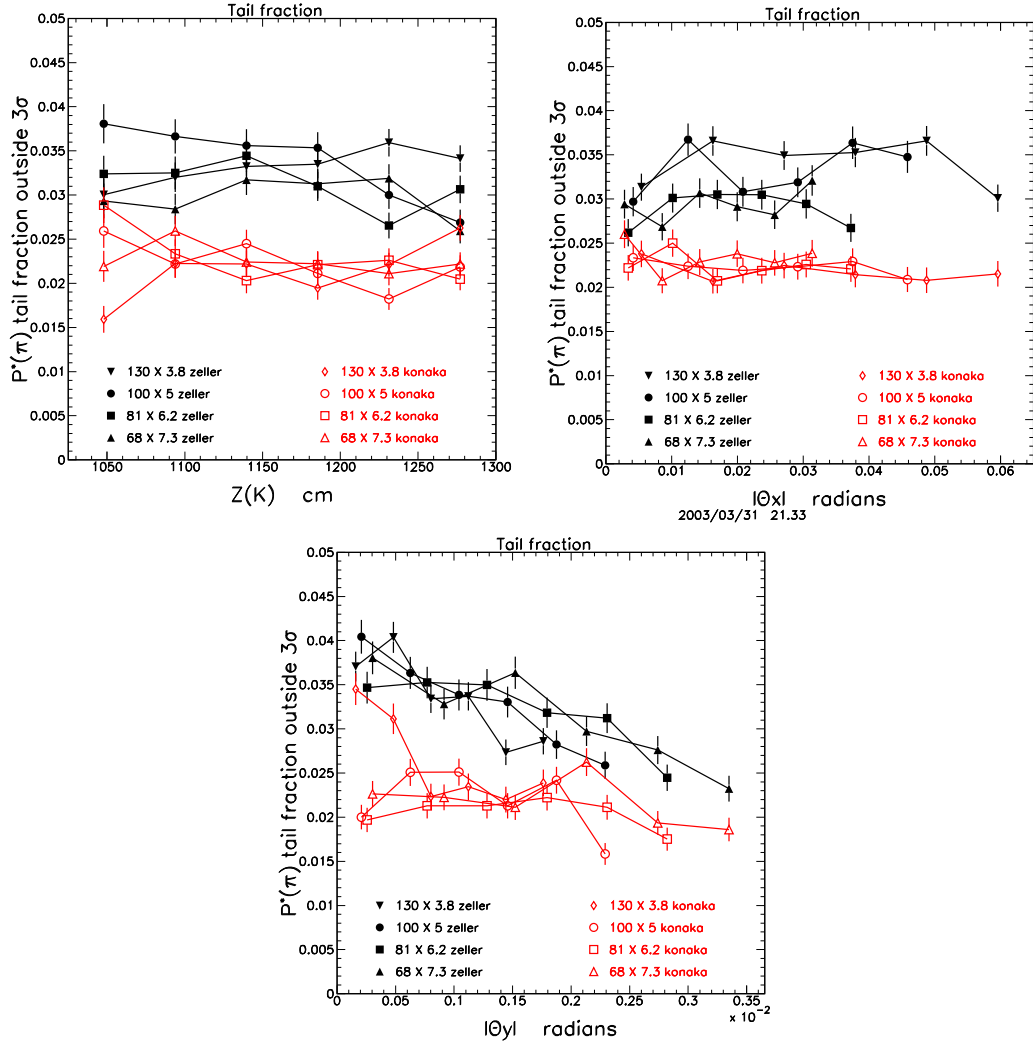


Figure 2: Fraction of  $P^*(\pi^0)$  distribution outside three  $\sigma$  where  $\sigma =$  core resolution as a function of  $Z(K)$ ,  $|\Theta_X|$  and  $|\Theta_Y|$  for the Konaka and Zeller PR models for the four different beam aspect ratios after application of basic cuts.

2003/03/31 21.34

2003/03/31 21.34

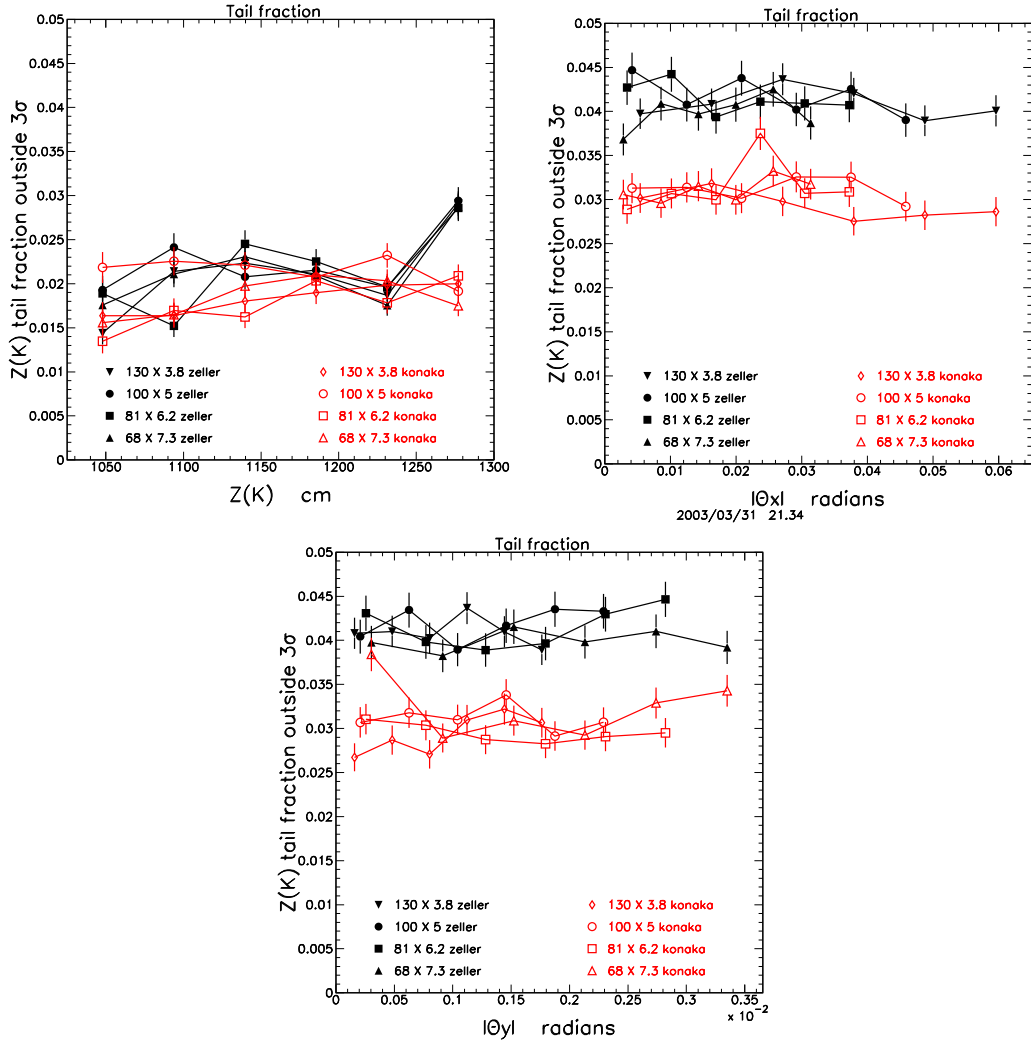


Figure 3: Fraction of  $Z(K)$  distribution outside three  $\sigma$  where  $\sigma =$  core resolution as a function of  $Z(K)$ ,  $|\Theta_X|$  and  $|\Theta_Y|$  for the Konaka and Zeller PR models for the four different beam aspect ratios after application of basic cuts.

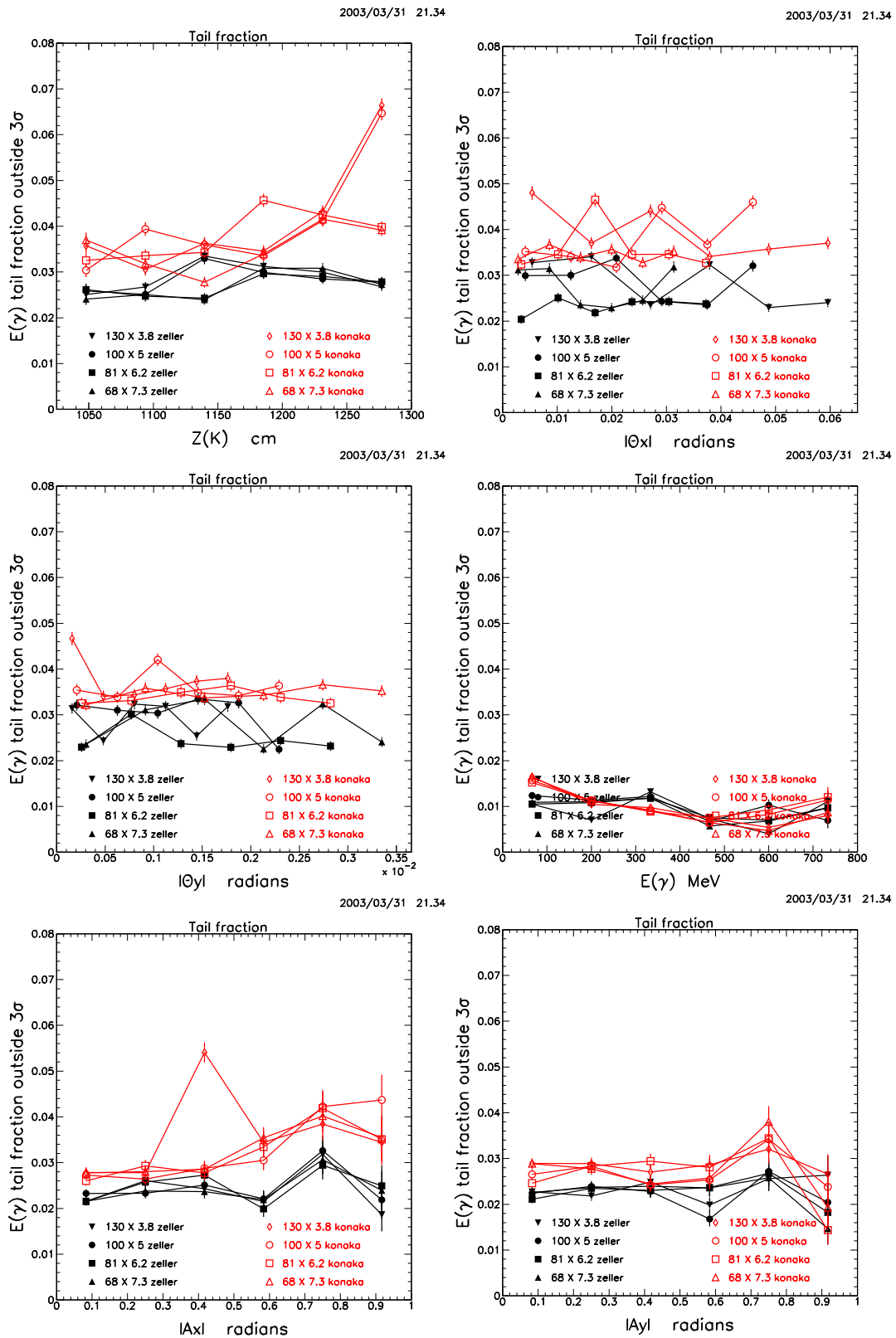


Figure 4: Fraction of  $E(\gamma)$  distribution outside three  $\sigma$  where  $\sigma =$  core resolution as a function of  $Z(K)$ ,  $|\Theta_X|$ ,  $|\Theta_Y|$ ,  $E(\gamma)$ ,  $|A_X|$  and  $|A_Y|$  for the Konaka and Zeller PR models for the four different beam aspect ratios after application of basic cuts.

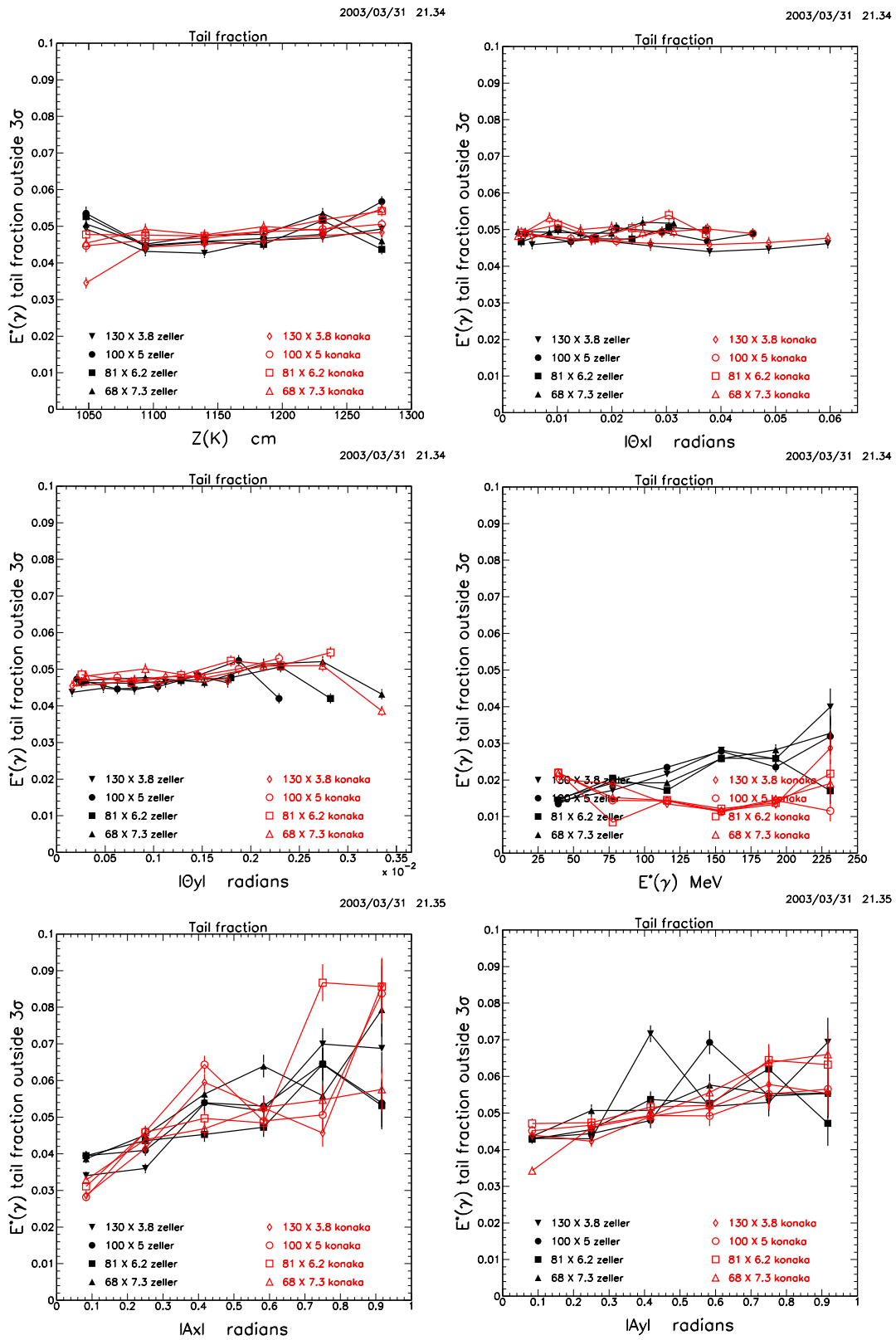


Figure 5: Fraction of  $E^*(\gamma)$  distribution outside three  $\sigma$  where  $\sigma =$  core resolution as a function of  $Z(K)$ ,  $|\Theta_X|$ ,  $|\Theta_Y|$ ,  $E^*(\gamma)$ ,  $|A_X|$  and  $|A_Y|$  for the Konaka and Zeller PR models for the four different beam aspect ratios after application of basic cuts.

## 2 Resolution and vertical beam constraint

Figures 7, 8, 9, 10 and 11 shows the  $M(\gamma\gamma)$ ,  $P^*(\pi^0)$ ,  $Z(K)$ ,  $E(\gamma)$  and  $E^*(\gamma)$  core resolutions, respectively, with and without the vertical beam constraint in the fit for the  $68 \times 7.3 \text{ mrad}^2$  aspect ratio and the Zeller PR model. The basic cuts described in TN053 have been applied.

The effect of the vertical beam constraint on the reconstructed vertical position of the  $K_L^0$  is shown in Figure 6.

Removing the constraint degrades the  $M(\gamma\gamma)$  core resolution to  $\sim 13 \text{ MeV}/c^2$ , independent of  $K_L^0$  production angle and decay point. The  $M(\gamma\gamma)$  resolution with the constraint varies from 11.4 to 12.4  $\text{MeV}/c^2$  depending on the production angle.

The  $P^*(\pi^0)$  resolution degrades to  $\sim 11 \text{ MeV}/c$  when the constraint is removed, compared to resolution in the range 9 to 10.5  $\text{MeV}/c$  with the constraint.

The constraint produces only a marginal improvement in the  $E^*(\gamma)$  resolution as a function of the vertical angle of the photon.

There is no change in the  $Z(K)$  and  $E(\gamma)$  when the constraint is removed.

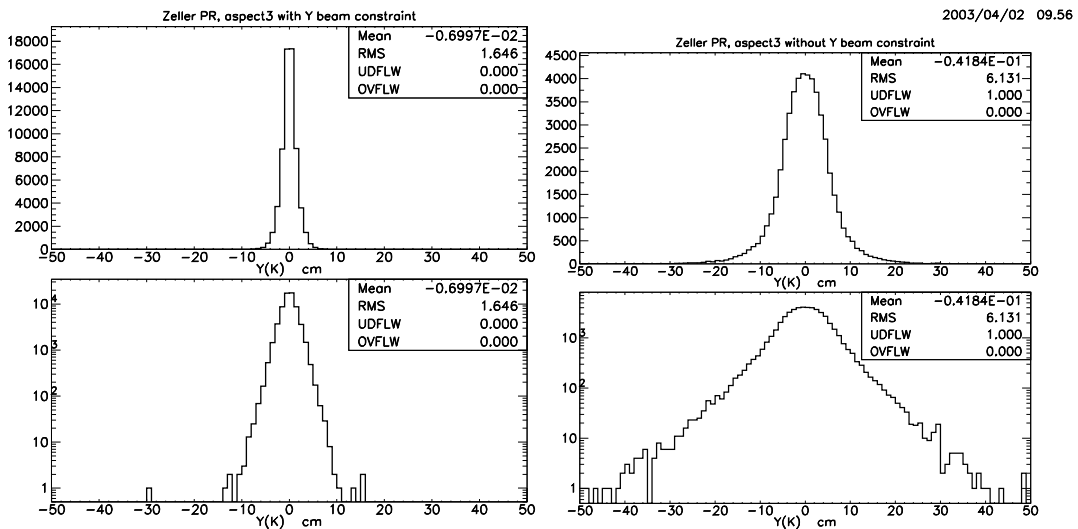


Figure 6: The reconstructed  $Y(K)$  for the Zeller PR model with the  $68 \times 7.3 \text{ mrad}^2$  aspect ratio. The left column shows the results of the fit with the vertical beam constraint. No vertical beam constraint is imposed for the distributions in the right column.

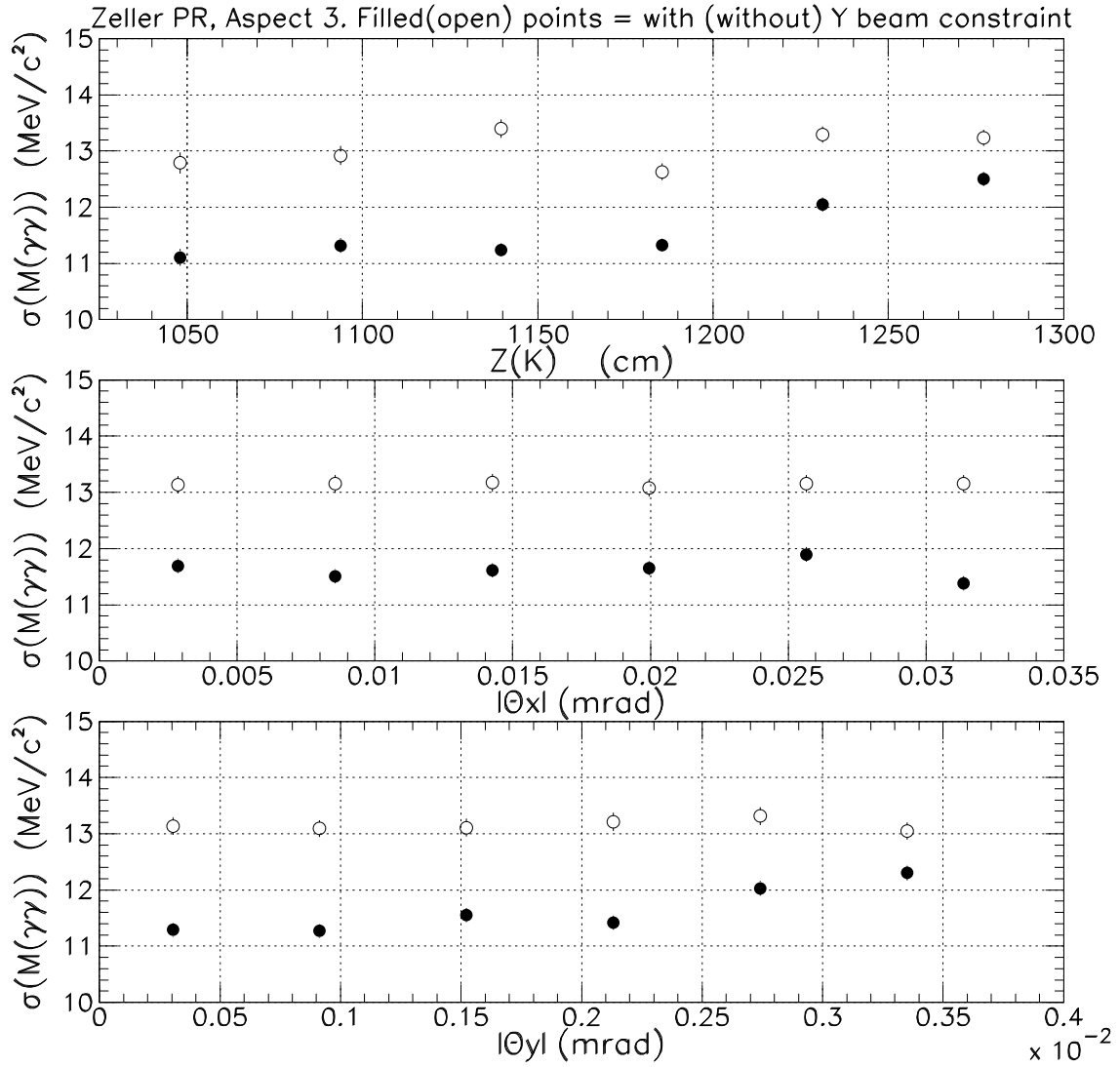


Figure 7: Core resolution on  $M(\gamma\gamma)$  as a function of  $Z(K)$ ,  $|\Theta_x|$  and  $|\Theta_y|$  for the Zeller PR model with the  $68 \times 7.3$  mrad<sup>2</sup> aspect ratio. The filled circles are the results of the fit with the vertical beam constraint. No vertical beam constraint is imposed in the fit for the open circles.

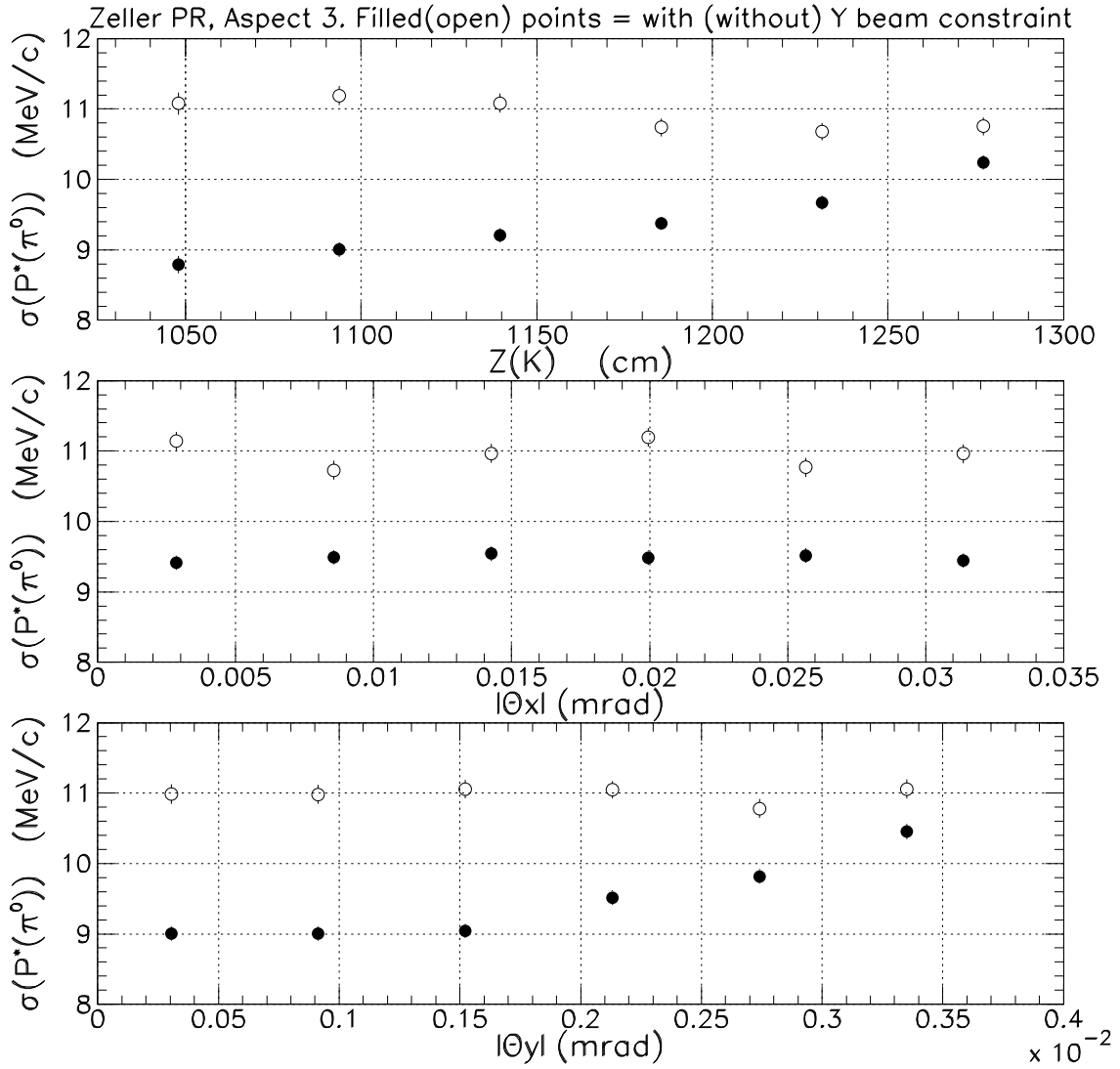


Figure 8: Core resolution on  $P^*(\pi^0)$  as a function of  $Z(K)$ ,  $|\Theta_X|$  and  $|\Theta_Y|$  for the Zeller PR model with the  $68 \times 7.3 \text{ mrad}^2$  aspect ratio. The filled circles are the results of the fit with the vertical beam constraint. No vertical beam constraint is imposed in the fit for the open circles.

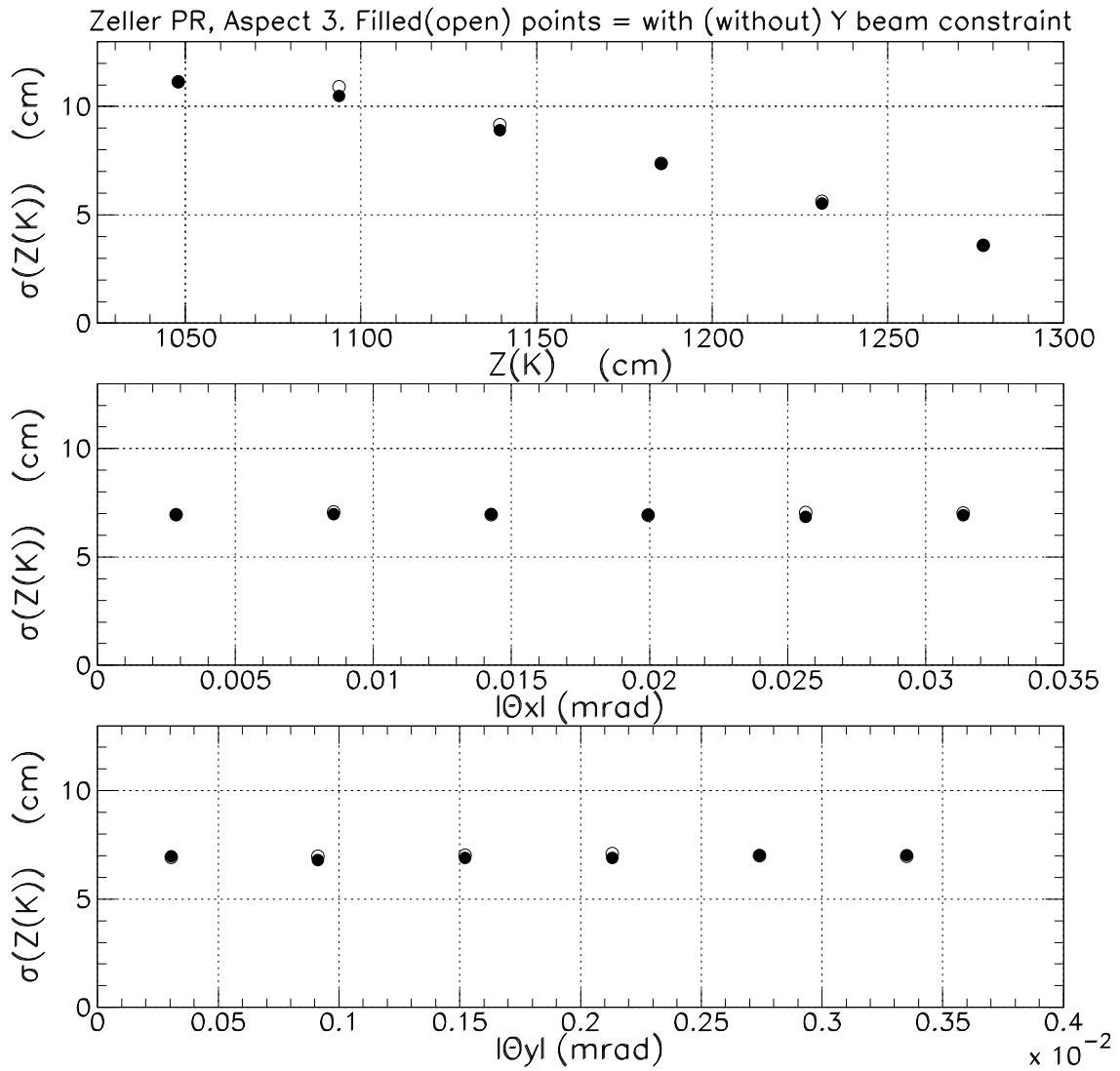


Figure 9: Core resolution on  $Z(K)$  as a function of  $Z(K)$ ,  $|\Theta_X|$  and  $|\Theta_Y|$  for the Zeller PR model with the  $68 \times 7.3 \text{ mrad}^2$  aspect ratio. The filled circles are the results of the fit with the vertical beam constraint. No vertical beam constraint is imposed in the fit for the open circles.

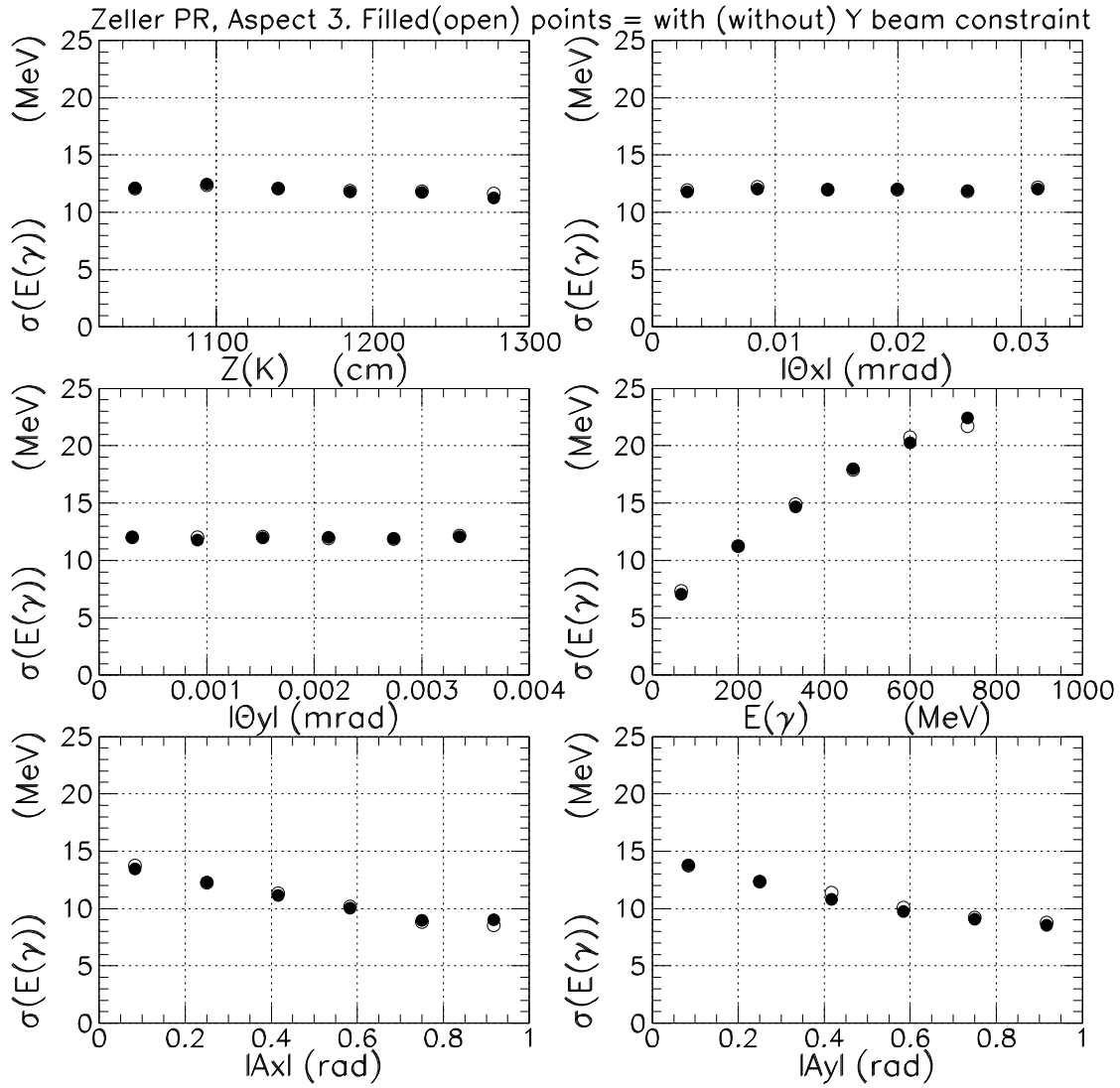


Figure 10: Core resolution on  $E(\gamma)$  as a function of  $Z(K)$ ,  $|\Theta_X|$ ,  $|\Theta_Y|$ ,  $E(\gamma)$ ,  $|A_X|$  and  $|A_Y|$  for the Zeller PR model with the  $68 \times 7.3$  mrad<sup>2</sup> aspect ratio. The filled circles are the results of the fit with the vertical beam constraint. No vertical beam constraint is imposed in the fit for the open circles.

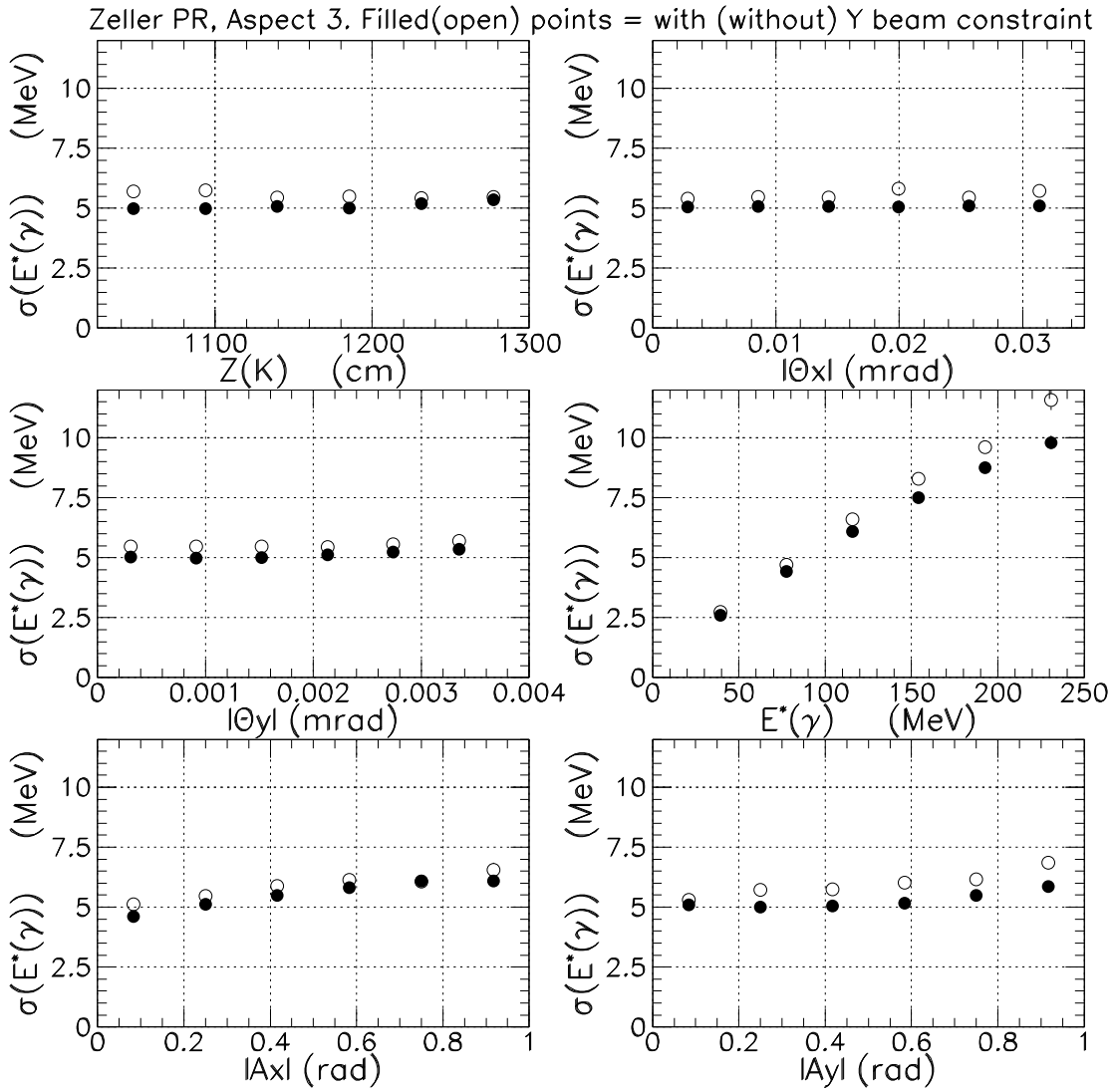


Figure 11: Core resolution on  $E^*(\gamma)$  as a function of  $Z(K)$ ,  $|\Theta_X|$ ,  $|\Theta_Y|$ ,  $E^*(\gamma)$ ,  $|A_X|$  and  $|A_Y|$  for the Zeller PR model with the  $68 \times 7.3 \text{ mrad}^2$  aspect ratio. The filled circles are the results of the fit with the vertical beam constraint. No vertical beam constraint is imposed in the fit for the open circles.